Acoustic Microscopy: A Study of Contrast in Fresh Tissue

Gail Scherba, Patricia A. Hoagland, and William D. O'Brien, Jr., *Fellow, IEEE*

Abstract— **The scanning laser acoustic microscope (SLAM), which exhibits a resolution of about 15 μm in biological materials, was operated at a frequency of 100 MHz to evaluate the source of image contrast. Specifically, the SLAM's quantitative capabilities yielded the ultrasonic propagation properties of attenuation coefficient and propagation speed of rat brain tissue (white versus gray matter) and these properties were correlated with tissue constituents and image contrast. The SLAM's image contrast between the two brain layers in both fresh and fixed specimens was analyzed subjectively by an experienced microscopist. It was determined that ethanol fixation decreased the image contrast between the brain layers. Additionally, the propagation speed was the least affected property in the fresh tissue specimens yet increased in both brain layers after fixation whereas the attenuation coefficient of white matter in unfixed brain tissue was higher than that of gray matter. These results indicate that the SLAM's acoustic image contrast is a direct reflection of the difference in attenuation coefficient whereas the propagation speed is not a significant contributor to the image contrast.**

I. Introduction

ONE OF THE general classes of acoustic microscopes is the scanning laser acoustic microscope (SLAM, Sonoscan, Bensenville, IL), which was developed in the early 1970's. The SLAM, which operates at frequencies between 10 MHz and 500 MHz, exhibits resolution capability in the 3 to 150 μm range. However, resolution is not the only benchmark to judge system capability. The SLAM also provides real-time (TV frame rate) image capability. In addition, it has proven quantitative potential with the ability to yield an attenuation coefficient and a propagation speed through specimens under study. In this regard, the SLAM's quantitative capability has not been completely documented in terms of the affect various specimen constituents have on the image contrast and therefore on the attenuation coefficient and propagation speed.

The goal of this paper is to evaluate the quantitative acoustic properties of animal tissue that affect image contrast. Specifically, the correlation between the ultrasonic propagation properties with tissue constituents and image constrast are the basis of the evaluation. The brain is used as the specimen due to its grossly visible and known tissue constituent differences between gray and white matter.

It is know that white and gray matter regions of the brain differ in cell structure and composition. The outermost layer of the cerebrum (upper portion of the brain) consists of gray matter, which contains the neuronal cell bodies, dendrites, the unmyelinated proximal portion of the axons, and nonneuronal supportive cells (neuroglia). In contrast, the white matter, which lies beneath the gray matter in this region, contains the conductile components, the myelinated axons, and sparse neuroglia, but is devoid of neuronal cell bodies. Therefore, the white matter contains a preponderance of myelin, composed of lipid substances, as compared to the more densely cellular gray matter. While there is a lipid component present in the cell membrane of all cells, the myelin sheaths have a higher lipid content than other portions of the brain. Additionally, white matter has a lower water content than gray matter. Tissue water content is known to affect both attenuation coefficient and propagation speed. Perturbation of this tissue component through dehydration (ethanol fixation) may decrease the apparent image contrast differences between the two brain layers.

The SLAM evaluation of rat brain tissue reveals image contrast differences between the two layers. Therefore, this study is designed to determine which tissue components are responsible for the SLAM's contrast. A second objective is to determine how tissue ultrasonic propagation properties (attenuation coefficient and propagation speed) are related to variations in the observed image contrast. It is suggested that the contrast is a direct reflection of the difference in attenuation coefficient, not propagation speed, and that the lipid content is a significant contributor to the attenuation coefficient.

II. Materials and Methods

A. Tissue Preparation

The brains from twelve 90 to 120 days old male Sprague-Dawley rats were used. The rats were euthanized humanely by an intraperitoneal injection of 0.5 ml sodium pentobarbital (50 mg/mL). The brain was removed, placed in chilled (4°C) isotonic saline and stored at 4°C for no more than 24 hours before either acoustic microscope evaluation or placement into fixative. The removed cerebrum was divided along the longitudinal fissure and a portion of the cerebrum was immediately mounted on a chuck for sectioning by a microtome (Vibratome Series 1000 Sectioning System, Technical Products International, Inc., St. Louis, MO) using cyanoacrylate adhe-

Manuscript received September 14, 1993; revised january 27, 1994; accepted January 31, 1994. This work was supported in part by the National Institutes of Health and National Cancer Institute by Grants CA09067 and CA39704

G. A. Scherba is with the Department of Veterinary Pathobiology, College of Veterinary Medicine, University of Illinois, Urbana, IL 61801 USA.

P. A. Hoagland was with the Department of Veterinary Pathobiology, College of Veterinary Medicine, University of Illinois, Urbana, IL. She is now with Amber Leaf Veterinary Clinic, Windfield, IL 60190 USA.

W. D. O'Brien, Jr. is with the Department of Electrical and Computer Engineering, University of Illinois, Urbana, IL 61801 USA.

IEEE Log Number 9401978.

sive. The mounted cerebrum for each animal was sectioned perpendicular to the longitudinal fissure at thicknesses of 250, 350, 500, 600, 700, and 900 μm, as based on and assumed to be within ± 20 μm of the microtome setting. The set of six thicknesses was maintained in normal saline (300 mOs) and served as a reference sample (untreated, time = 0). The other sets were fixed by incubation in 80% ethanol (EtOH; adjusted to 300 mOs with saline) at 4°C from 1 to 53 h. After the specified times in EtOH, the sections were removed, placed in normal saline and stored at 4°C for no more than 24 hours before acoustic microscope evaluation. Adjustment of the EtOH to isotonicity was done to stabilize ion concentrations within the tissues. An 80% EtOH solution was used to avoid excessive shrinkage that could result in morphological distortions. Storage of the specimens in normal saline after fixation was done to prevent excessive hardening of the tissue [1].

B. Acoustic Microscopy

For acoustic microscopy evaluation, the sectioned cerebral tissue was trimmed to the dimensions of 2.5 mm by 1.5 mm. It then was transferred to the microscope stage using a fine camel hair brush and covered with a thin layer of normal saline. A ring spacer of appropriate thickness supported a semi-reflective coverslip placed over the submerged specimen. The evaluations were conducted at room temperature ($\approx$ 22°C)

A SLAM (Sonomicroscope 100® Sonoscan, Inc., Benesenville, IL), operating at an ultrasonic frequency of 100 MHz, was used to determine the specimen's attenuation coefficient and propagation speed. Operational details of the SLAM have been published previously [2]–[10]. Briefly, the SLAM produces an acoustic image, from which the attenuation coefficient is determined, and an interference image, from which the propagation speed is calculated. Both images, displayed in real-time on a standard television monitor, represent a specimen area of approximately 3 mm horizontally by 2 mm vertically (typically 100×). A frame grabber digitized (8 bit) the video signal of the acoustic and interference images [9] and performed frame averaging (up to 256 frames), convolutions (for filtering), and histograms (for dynamic range determination). Attenuation coefficient and propagation speed estimations were quantified by software utilizing the digitized video images.

An insertion loss procedure was employed to estimate the attenuation coefficient [3], [8]. In principle, this procedure compares the received signal amplitude of the specimen of known thickness in the sound path with that of the reference medium, normal saline. A subimage area of approximately 400 μm $\times$250 μm (96 pixels horizontally by 32 pixels vertically) in the acoustic image was used. The signals received from the subimage area were digitized to yield an average amplitude value (V). A minimum of five V values were recorded for normal saline, the reference medium. The tissue specimen then was moved into the subimage area and a minimum of five values of V were recorded at each of five separate specimen locations within each of the two brain tissue regions. An insertion loss (IL) value, in dB, was estimated from:

$$\mathrm{IL} = V_s - \langle V_r \rangle \tag{1}$$

where $\langle V_r \rangle$ is the mean value of V recorded from normal saline, the reference medium, and V_s are individual values of V from the specimen. This process yielded five IL values for each specimen thickness from adjacent spatial regions. Six specimen thicknesses ranging from 250 μm to 900 μm were used and the slope of IL versus specimen thickness, *via* a linear least-squares fit (utlilzing all 30 IL-thickness values), yielded the attenuation coefficient.

The spatial frequency domain technique was used to yield speed from the interference image [4], [8]. The 2 mm $\times$ 3 mm field of view contained approximately 39 vertical interference lines equally space by about 85 μm. The propagation speed was estimated by the horizontal shift of the fringe lines relative to where the fringe lines would be without the specimen, that is, relative to the reference (known speed value) medium. The specimen was positioned such that each interference line includes both the reference fluid above and below the specimen and the specimen. From the digitized interference image, each interference line was digitized and processed yielding a vertical (relative to the image orientation) speed profile. For each sample, six specimen thicknesses were analyzed, each yielding a mean speed value from the speed profile regional within the specimen. The individual mean speed values were averaged to yield the propagation speed of that sample.

Image contrast directly from the SLAM monitors was analyzed subjectively by an experienced microscopist in terms of whether the boundary between gray and white matter could be detected.

C. Uncertainties

Specimen thickness uncertainty of ± 20 μm for all of the Vibratome settings would result in propagation speed uncertainties of 0.3 and 0.1% at specimen thicknesses of 250 and 900 μm, respectively and in an attenuation coefficient uncertainty of 7% [8].

Uncertainty of the estimates of attenuation coefficient and propagation speed from the SLAM have been assessed for solutions of known acoustic properties [8]. Using a homogenous medium, the accuracy (proximity to the true value) was $\pm 2.9\%$, and the precision (reproducibility of successive independent measurements) was $\pm 0.4\%$ for propagation speed; and for attenuation coefficient, accuracy and precision were $\pm 12\%$ and $\pm 15\%$, respectively.

Therefore, propagation speed and attenuation coefficient measurement uncertainties are estimated to be 0.5% ($\sqrt{0.3^2 + 0.4^2}$) and 17% ($\sqrt{7^2 + 15^2}$), respectively.

III. Results

A total of twelve brains were studied of which ten were evaluated for propagation speed, six were evaluated for attenuation coefficient and four were evaluated for both propagation speed and attenuation coefficient.

Fig. 1 shows an example of the two types of images (top: acoustic; bottom: interference) obtained from the SLAM

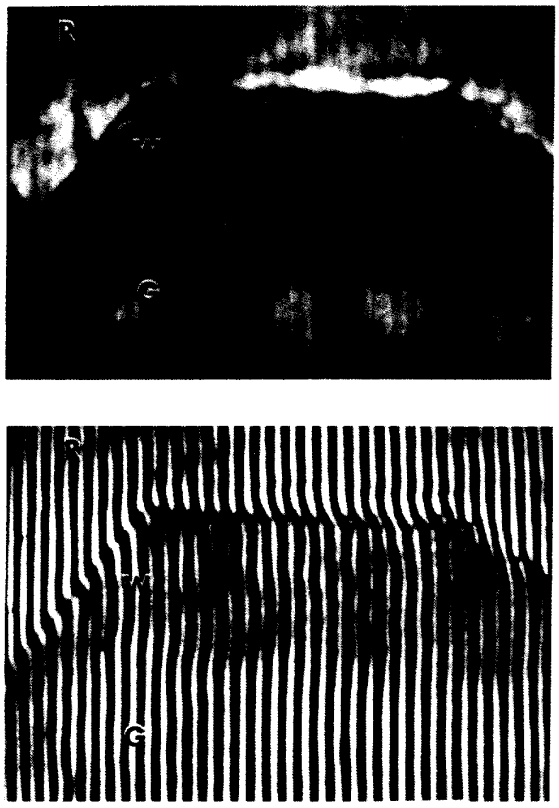

Fig. 1. Photographs from the SLAM monitor of (top) acoustic image and (bottom) interference image for a region of fresh, unfixed (time = 0) cerebrum which contains both white and gray matter along with the reference saline. R: saline reference, W: white matter, G: gray matter.

for a region of unfixed, fresh cerebrum which contains both white and gray matter along with the reference saline. An experienced microscopist evaluated contrast between gray and white matter visually and subjectively from the acoustic image directly off of the SLAM monitors. Twelve animal brains for various EtOH fixation durations (0, 1, 3, 4, 5, 6, 7, 12, 24, 30 and 53 h) were evaluated from both the acoustic and interference image. The white matter is the more attenuating region in unfixed brain as indicated by the relative brightness levels between white (darker appearance) and gray matter (Fig. 1, top). This was a consistant observation for the five unfixed brains that were evaluated (EtOH fixation duration of 0 h). The vertical interference lines (Fig. 1, bottom) shift to the right as the sound wave passes from the reference saline at the top of the interference image into white matter and then shift very slightly to the left as the wave passes from white matter into gray matter suggesting that the white matter has a slightly greater speed than the reference and gray matter. Following fixation, the contrast between white and gray matter diminishes. The diminution of contrast was noticable within the first few hours of fixation and was completely absent after 24 h of fixation.

Of the twelve brains studied, quantitative evaluations of propagation speed were conducted in ten at various EtOH fixation durations (Fig. 2). Nine of the brains were evaluated

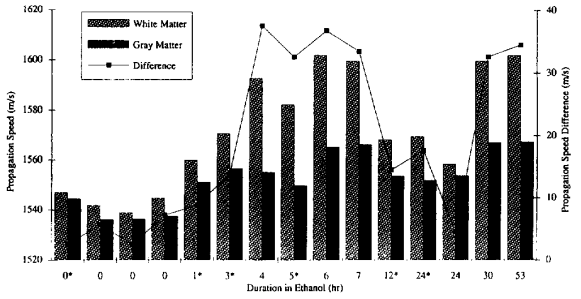

Fig. 2. Individual observations of the propagation speed as a function of fixation duration in ethanol for gray and white matter from ten animals, one of which was evaluated at six fixation durations (*). The solid line connects points which represent the difference between gray and white propagation speed.

at a single EtOH fixation duration and one at six durations. For unfixed tissue (time = 0), the propagation speeds for white and gray matter are almost the same (Fig. 2), that is, within the measurement uncertainty. The speed for white matter increases as the function of fixation duration, decreases slightly and then increases at the longest fixation durations whereas, for gray matter, there is a slight overall increase in speed with increased fixation duration. The difference between white and gray matter propagation speed values is greater for the fixed tissues compared to unfixed, fresh tissue.

The four speed values for unfixed white matter were within 0.26% of the mean value ($\langle$ 1543 m/s$\rangle$, range: 1539–1547 m/s) and for the unfixed gray matter within 0.39% of the mean value ($\langle$ 1539 m/s$\rangle$, range: 1536–1545 m/s). The two speed values for 24-hour fixed white and gray matter were within 0.38 and 0.06% of their mean values ($\langle$1564 m/s$\rangle$, range: 1559–1570 m/s and $\langle$1553$\rangle$, range: 1552–1554 m/s), respectively. These results are within the speed measurement uncertainty of $\pm 0.5\%$ and therefore a measurement uncertainty of $\pm 0.5\%$ is assigned to all measures, individual and averaged. The measurement uncertainty of the propagation speed difference between white and gray matter is calculated from $\sqrt{(\delta w)^2 + (\delta g)^2}$ where δw and δg are the measurement uncertainties (based on 0.5% of the measured individual or averaged observations) of white and gray matter propagation speed measurements, respectively. Fig. 3 shows graphically the propagation speed difference $\pm$ measurement uncertainty as a function of duration in EtOH for the averaged (unfixed and 24-hour fixed) and individual observations.

Of the twelve brains studied, quantitative evaluations of attenuation coefficient were conducted in six at various EtOH fixation durations (Fig. 4). Five of the brains were evaluated at a single EtOH fixation duration and one at six durations. The attenuation coefficient for unfixed white matter is about two times greater than for gray matter. The attenuation coefficient for both gray and white matter increases as a function of fixation time and then decreases. After 24 h of fixation, the attenuation coefficients for these two tissue types are almost identical.

The four attenuation coefficient values for unfixed white matter were within 12.2% of the mean value ($\langle$81.7 dB/cm$\rangle$,

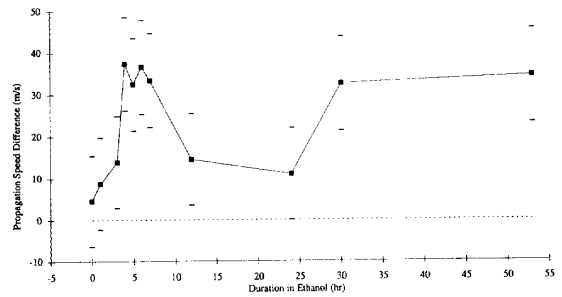

Fig. 3. Individual and averaged observations of the propagation speed difference as a function of fixation duration in ethanol for gray and white matter. The horizontal lines above and below the data points are the ± measurement uncertainties. The horizontal dashed line shows zero speed difference.

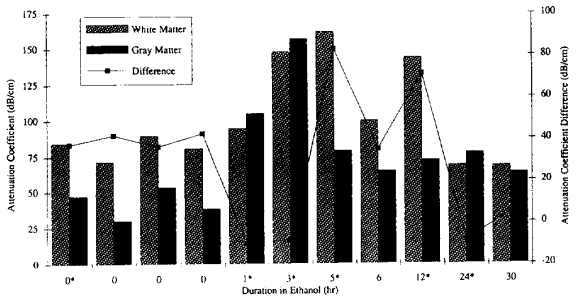

Fig. 4. Individual observations of the attenuation coefficient as a function of fixation duration in ethanol for gray and white matter from six animals, one of which was evaluated at six fixation durations (*). The solid line connects points which represent the difference between gray and white attenuation coefficient.

range: 71.8–89.7 dB/cm) and for the unfixed gray matter with 28.8% of the mean value (⟨42.4 dB/cm⟩, range: 30.2–53.4 dB/cm). These white matter results are within the attenuation coefficient measurement uncertainty of ±17% and therefore a measurement uncertainty of ±17% is assigned to all individual and white matter averaged observations, whereas a measurement uncertainty of ±29% is assigned to the gray matter averaged observation. The measurement uncertainty of the attenuation coefficient difference between white and gray matter is calculated from $\sqrt{(\delta w)^2 + (\delta g)^2}$ where δw and δg are the measurement uncertainties (based on 17% of the measured individual or white matter averaged observation and 29% of the measured gray matter averaged observation) of white and gray matter attenuation coefficient measurements, respectively. Fig. 5 shows graphically the attenuation coefficient difference ± measurement uncertainty as a function of duration in EtOH for the averaged (unfixed) and individual observations.

IV. Discussion

A. Acoustic Contrast

Acoustic contrast of SLAM images refers to the acoustic image, not the interference image (see Fig. 1). There are two general phenomena which can be attributed to acoustic image contrast, that is, the ability to visualize boundaries between

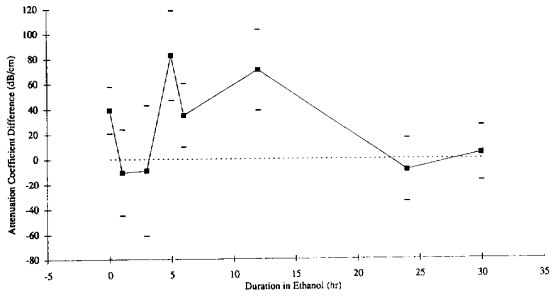

Fig. 5. Individual and average dobservations of the attenuation coefficient difference as a function of fixation duration in ethanol for gray and white matter. The horizontal lines above and below the data points are the ± measurement uncertainties. The horizontal dashed line shows zero attenuation coefficient difference.

two regions such as between gray and white matter. If two tissue regions exhibit different attenuation coefficients, then the region with the higher attenuation coefficient will appear darker than the other because of the differential propagated loss. On the other hand, if two regions exhibit different characteristic acoustic impedances (defined as the product of density and propagation speed), then the ultrasonic energy propagated into the two regions will be different at the stage-tissue interface because of the dissimilar differential characteristic acoustic impedances between the stage and tissue.

B. Ultrasonic Propagation Property and Tissue Constituent Behavior

Qualitative and quantitative relationships exist between the ultrasonic propagation properties (attenuation coefficient and propagation speed) and certain tissue constituents [5]–[7], [10]–[16]. Since ultrasonic propagation properties are largely determined at the macromolecular level [17]–[19] and can be quantitatively measured using the SLAM, this microscope can therefore be utilized to image the mechanical properties of tissue. Such mechanical properties are a characteristic of the tissue constituents (water, lipid, and protein) and their amounts.

Attenuation includes absorption (loss of energy into heat) and scattering (redirection of the energy due to heterogeneity within the specimen). Scattering includes reflection, refraction and diffraction. These two components of ultrasonic propagation, absorption and scattering, define the attenuation coefficient as a measure of the decrease in energy of the sound wave as it propagates through material. The remaining component of ultrasonic propagation, the propagation speed, provides information on the microscopic elastic properties of a tissue.

The ultrasonic attenuation of water is well below that of soft tissues, although its ultrasonic speed is comparable to but slightly less than that of soft tissues. Hence, tissues containing larger amounts of water, e.g., testes and fetal brain, exhibit a relatively low attenuation coefficient and slightly lower speed, respectively [13]–[15]. Both attenuation coefficient and speed decreases as tissue water concentration increases [6]–[7],

[10]–[12]. As tissue lipid concentration increases, it has been reported that the attenuation coefficient increases and speed decreases [5], [7], [12]. Proteins seem to be responsible for the largest part of the observed tissue attenuation [16] although changes in tissue protein concentration (with the exception of structural proteins) have not exhibited significant effects on either attenuation coefficient or speed [7]. Thus, these general trends can be viewed as follows:

$$\text{When water } \Uparrow \text{ or lipid } \Downarrow, \text{attenuation coefficient } \Downarrow \quad (2)$$

$$\text{When water } \Downarrow \text{ or lipid } \Downarrow, \text{ propagation speed } \Uparrow \quad (3)$$

Attenuation coefficient and propagation speed were measured for portions of fresh rat brain that represented areas of white and gray matter. Gray matter is denser than white matter and has a higher water content and a lower lipid content [20], that is

$$\text{White matter: Less dense Less water More lipid} \quad (4a)$$

$$\text{Gray matter: More dense More water Less lipid} \quad (4b)$$

The gray matter in the outer regions of the cerebrum contains neuron cell bodies, their attached dendritic arborization and supporting cells, the protoplasmic astrocytes. White matter is composed of axons, myelinated by oligodendrocytes and supported by fibrillary astrocytes. Microtubules, neurofilaments (intermediate filaments), and microfilaments, protein polymers present in the neurons are more conspicuous in axons. The fibrillary astrocytes of white matter display long, straight processes and contain more abundant fibrils in their cytoplasm than the protoplasmic astrocytes of gray matter [21], [22].

C. Fresh, Unfixed Tissue

In previous studies [5], [12], propagation speed had been shown to decrease with increasing lipid or water content of tissue. In this study, the propagation speed through white matter tract regions was very slightly higher than that through the cortical gray matter (see Fig. 2) which is consistent with the fact that the white matter tracts contain a lesser amount of water than the gray matter, but inconsistent with the higher amount of lipid. This would suggest that water content has a more dominant effect on propagation speed than does lipid content in fresh, unfixed tissue. Further, the propagation speed difference (see Fig. 3), when measurement uncertainity is taken into account, suggests that there is no difference for individual propagation speed measurements. Thus, acoustic image contrast between white and gray matter for fresh, unfixed brain tissue does not appear to dependent upon differential propagation speed. Also, the acoustic impendance differences between white and gray matter could be considered negligible because the very slightly higher propagation speed of white matter, when multiplied by the slightly lower density, would yield a characteristic acoustic impedance value quite similar to that of gray matter (product of slightly lower propagation speed and slightly higher density).

Also, in previous studies [5], [7], [10], [11], it was determined that the attenuation coefficient is directly proportional to the lipid and inversely proportional to water content of a tissue, so that increasing lipid concentration or decreasing water concentration will cause an increase tissue attenuation coefficient. It was determined that white matter tracts adjacent to the lateral and third ventricles possessed a significantly greater attenuation coefficient as compared with the gray matter regions of the cortex, the outer layer of the cerebrum (see Fig. 4). The attenuation coefficient difference (see Fig. 5), when measurement unceratinty is taken into account, suggests that there is a difference for individual attenuation coefficient measurements. This is consistent with the fact that white matter tracts contain a higher amount of lipids and a lower amount of water than the gray matter. Therefore, it is apparent that either water content and/or lipid content has a dominant effect on attenuation coefficient in fresh, unfixed tissue. Consequently, acoustic image contrast between white and gray matter for fresh, unfixed brain tissue does appear to dependent upon differential attenuation coefficient.

The results from this study indicate that the lipid content differences in various regions of the brain are characterizable by the acoustic microscope for certain ultrasonic propagation properties, speed and attenuation coefficient. Therefore, the SLAM may have general application in differentiating the structural or compositional property of a tissue, in this case fresh, unfixed rat brain, as it contributes to differences in acoustic properties within the tissue.

D. Intermediate EtOH Fixation Duration

Ethanol was chosen as a fixative because of its rapid penetration, effective dehydration and protein denaturation characteristics. These characteristics help preserve water soluble components in their appropriate locations. Alcohol protein denaturation is affected by simple *in situ* coagulation rather than cross-linking thereby imparting rigidity to the tissue so that the shape of the tissue is maintained during sectioning. In addition, EtOH is a mediocre lipid solvent and so should not greatly alter this component of the white matter [1].

The intermediate EtOH fixation duration behavior of the ultrasonic propagation properties must be view a little different for propagation speed and attenuation. Propagation speed appears to have reached a steady-state behavior at 30-hour EtOH fixation duration (see Figs. 2 and 3) whereas attenuation coefficient appears to reach a steady-state behavior at 24-hour EtOH fixation duration (see Figs. 4 and 5). There does not appear to be an explanation as to why there is an apparent difference between the times required to reach steady-state since the time course of the fixation process is unknown. Also, unknown is why the acoustic contrast is lost for EtOH fixation times between five and twelve hours when both propagation speed and attenuation coefficient differences exhibit significant differences. In general, as a function of EtOH fixation time, there is a slight decrease in lipid content, a decrease in water content and an increase in protein coagulation. The strength

of each of these effects upon the ultrasound propagation properties remains to be determined.

Within the first couple of hours of fixation, as some of the lipid and water are removed during the fixation process, propagation speed increased in both gray and white matter as expected (see (3)). Also, attenuation coefficient increased as expected if water were assumed to be the dominant contributor (see (2)) since the tread is opposite that expected for a decrease in lipid content. Yet, the acoustic contrast starts to diminish during the first couple of hours of fixation. During this time, the propagation speed difference becomes significant while the attenuation coefficient difference becomes negligible which supports the hypothesis that the attenuation coefficient is the principal acoustic image contrast determinant.

E. Steady-State EtOH Fixation Duration

It is assumed in steady-state EtOH fixation conditions that the water content between white and gray matter is much more similar than that for fresh, unfixed tissue and that the lipid content difference between white and gray matter is essentially the same as that for fresh, unfixed tissue. Under these conditions, the propagation speed of both white and gray matter increased significantly from that of fresh, unfixed tissue (see Fig. 2) as did the propagation speed difference (see Fig. 3). These observations suggest that the lipid content difference is the principal determinant since white matter has a greater lipid content and both white and gray matter have close to the same water content.

Also, under steady-state EtOH fixation conditions, the attenuation coefficient of white matter only slightly decreased from that of fresh, unfixed tissue whereas that of gray matter increased significantly (see Fig. 4) such that the attenuation coefficient difference was negligible (see Fig. 5). For white matter, this suggests that the tissue dehydration may be offset be some action of the protein coagulation since the lipid content did not change significantly. In contrast, the data indicates that the water content decrease could have been the principal determinant for gray matter.

In summary, it can be suggested that: i) the contrast observed in the acoustic image is a direct reflection of the difference in attenuation coefficient and ii) the propagation speed is not a significant contributor to the contrast. Further, it can be suggested that water and lipid content affect the ultrasonic propagation properties with both appearing to influence propagation speed and with water being the principal determinant influencing attenuation coefficient.

F. Literature Comparison of Fresh, Unfixed Brain Tissue

Finally, the ultrasonic propagation properties of the unfixed, fresh brain tissues are compared to the most of the world's literature [23],[24], all of which represents data obtained in the low ultrasonic frequency range (see Figs. 6 and 7). A regression analysis to a power law fit for the 76 attenuation coefficient versus frequency observations from in Fig. 6 yielded

$$A = 0.689 f^{1.003} \tag{5}$$

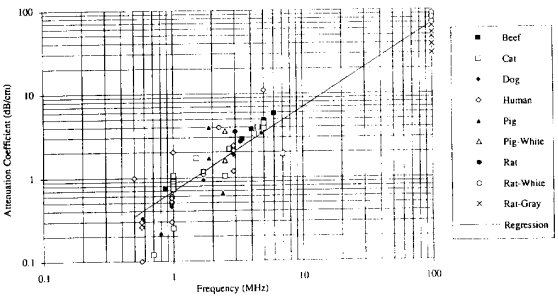

Fig. 6. Summary of attenuation coefficientas a function of frequency for brain tissue from several animal species. The solid line represents the regression (see (5)).

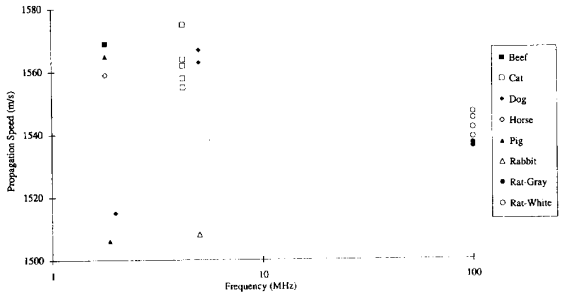

Fig. 7. Summary of propagation speed as a function of frequency for brain tissue from several animal species.

where A is the attenuation coefficient (in dB/cm), f is the ultrasonic frequency (in MHz) and where the regression analysis yielded an adjusted R^2 value of 0.89, a standard error value of 0.22 and a p value of 0.0001. For comparision, a similar regression analysis over the same frequency range for 116 measurements of fresh bovine liver yielded [25]

$$A = 0.373 f^{1.270} \tag{6}$$

The 21 propagation speed versus frequency observations (Fig. 7) indicate that the eight values obtained in this study with the SLAM lie within the range of the speed values obtained at the lower frequencies for other animals.

REFERENCES

[1] S. W. Thompson and R. D. Hunt, *Selected Histochemical and Histopathological Methods.* Springfield, IL: Charles C. Thomas, 1966, pp. 3–18.

[2] P. M. Embree, K. M. U. Tervola, S. G. Foster, and W. D. O'Brien, Jr., "Spatial distribution of the speed of sound in biological materials with the scanning laser acoustic microscope," *IEEE Trans. Sonics Ultrason.*, vol. SU-32, pp. 341–350, 1985.

[3] K. M. U. Tervola, S.G. Foster, and W.D. O'Brien, Jr., "Attenuation coefficient measurement technique at 100 MHz with the scanning laser acoustic microscope," *IEEE Trans. Sonics Ultrason.*, vol. SU-32, pp. 259–265, 1985.

[4] K. M. U. Tervola and W. D. O'Brien, Jr., "Spatial frequency domain technique: An approach to analyze the scanning laser acoustic microscope," *IEEE Trans. Sonics Ultrason.*, vol. SU-32, pp. 544–554, 1985.

[5] K. M. U. Tervola, M. A. Grummer, J. W. Erdman, Jr., and W. D. O'Brien, Jr., "Ultrasonic attenuation and velocity properties in rat liver as a function of fat concentration—A study at 100 MHz using a scanning laser acoustic microscope," *J. Acoust. Soc. Amer.*, vol. 77, pp. 307–313, 1985.

[6] J. E. Olerud, W. D. O'Brien, Jr., M. A. Reiderer-Henderson, D. L. Steiger, F. K. Forster, C. Daly, D. J. Ketterer, and G. F. Odland, "Ultrasonic assessment of skin and wounds with the scanning laser acoustic microscope," *J. Investigative Dermatol.*, vol. 88, pp. 615–623, 1987.
[7] W. D. O'Brien, Jr., J. W. Erdman, Jr., and T.B. Hebner, "Ultrasonic propagation properties (@100 MHz) in excessively fatty rat liver," *J. Acoust. Soc. Amer.*, vol. 83, pp. 1159–1167, 1988.
[8] D. L. Steiger, W. D. O'Brien, Jr., J. E. Olerud, M. A. Riederer-Herderson, and G. F. Odland, "Measurement uncertainty assessment of the scanning laser acoustic microscope and application to canine skin and wound," *IEEE Trans. Ultrason., Ferroelec., Freq. Contr.*, vol. 35, pp. 741–748, 1988.
[9] D. D. Nicozisin, "An automated image data acquisition and analysis stystem for the scanning laser acoustic microscope," M.S. degree Thesis, Dept. Electrical and Computer Eng., Univ. of Illinois, Urbana, 1989.
[10] K. B. Sagar, D. H. Agemura, W. D. O'Brien, Jr., L. R. Pelc, T. L. Rhyne, L. S. Wann, R. A. Komorowski, and D. C. Warltier, "Quantitative ultrasonic assessment of normal and ischaemic myocardium with an acoustic microscope: relationship to integrated backscatter," *Cardiovasc. Res.*, vol. XXIV, pp. 447–455, 1990.
[11] J. E. Olerud, W. D. O'Brien, Jr., M. A. Riederer-Henderson, D. L. Steiger, J. Debel, and G. F. Odland. "Correlation of tissue constituents with the acoustic properties of skin and wound," *Ultrasound in Med. and Biol.*, vol. 16, pp. 55–64, 1990.
[12] J. C. Bamber, C. R. Hill, and J. A. King, "Acoustic properties of normal and cancerous human liver—II. Dependence on tissue structure," *Ultrasound Med. Biol.*, vol. 7, pp. 135–144, 1981.
[13] J. W. Wladimiroff, I. L. Craft, and D. G. Talbert, "*In vitro* measurements of sound velocity in human fetal brain tissue," *Ultrasound Med. Biol.*, vol. 1, pp. 377–382, 1975.
[14] J. K. Brady, S. A. Goss, R. L. Johnston, W. D. O'Brien, Jr., and F. Dunn, "Ultrasonic propagation properties of mammalian testes," *J. Acoust. Soc. Amer.*, vol. 60, pp. 1404–1409, 1976.
[15] S. A. Goss, L. A. Frizzell, and F. Dunn, "Ultrasonic absorption and attenuation in mammalian tissues," *Ultrasound Med. Biol.*, vol. 5, pp. 181–186, 1979.
[16] F. Dunn and W. D. O'Brien, Jr., "Ultrasonic absorption and dispersion," in *Ultrasound: Its Application in Medicine and Biology*, F. J. Fry, Ed. The Netherlands: Elsevier, 1978, pp. 393–439.
[17] E. L. Carsentsen, K. Li, and H. P. Schwan, "Determination of the acoustic properties of blood and its components," *J. Acoust. Soc. Amer.*, vol. 25, pp. 286–289, 1953.
[18] E. L. Carsentsen and H. P. Schwan, "Acoustic propeties of hemoglobin solutions," *J. Acoust. Soc. Amer.*, vol. 31, pp. 305–309, 1959.
[19] H. Pauly and H. P. Schwan, "Mechanism of absorption of ultrasound in liver tissue," *J. Acoust. Soc. Amer.*, vol. 50, pp. 692–699, 1971.
[20] H. McIlwain, *Biochemistry and the Central Nervous System.* Boston, MA: Little, Brown and Co., 1959, p. 26.
[21] R. L. Davis and D. M. Robertson, *Textbook of Neuropathology.* Baltimore, MD: Williams & Wilkins, 1985, pp. 1–92.
[22] A. Peters, S. L. Palay, and H. Webster, *The Fine Structure of the Nervous System.* Philadelphia: W.B. Saunders, 1976, pp. 233–250.
[23] S. A. Goss, R. L. Johnson, and F. Dunn, "Comprehensive compilation of empirical ultrasonic properties of mammalian tissues," *J. Acoust. Soc. Amer.*, vol. 64, pp. 423–457, 1978.
[24] ———, "Compilation of empirical ultrasonic properties of mammalian tissues. II," *J. Acoust. Soc. Amer.*, vol. 68, pp. 93–108, 1980.
[25] J. D. Pohlhammer, C. A. Edwards, and W. D. O'Brien, Jr., "Phase insensitive ultrasonic attenuation coefficient determination of fresh bovine liver over an extended frequency range," *Med. Phys.*, vol. 8, pp. 692–694, 1981.

Gail Scherba received the D.V.M. and Ph.D. degrees in animal virology from Purdue University.

Since 1988 she has been an Assistant Professor of veterinary virology and Setion Chief of the Veterinary Virology Diagnostic Laboratory at the University of Illinois, Urbana. Her interests include basic and applied research on animal infectious diseases for which she uses molecular, classical, and epidemiological techniques. Her current research focus involves the genetic regulation of herpesviral latency. She is also involved in collaborative efforts in diverse research areas such as the understanding of how ultrasonic energy interacts with biological tissues for ultimate evaluation of viral-based diseases and the characterization of newly recognized viral diseases in both domestic and exotic animals.

Patricia A. Hoagland, photograph and biography not available at the time of publication.

William D. O'Brien, Jr. (S'64–M'70–SM'79–F'89), for a photograph and biography, see p. 301 of the May 1994 issue of this TRANSACTIONS.